FINAL TECHNICAL REPORT

Project Title:	NEER/ Developmemt of a Large-Field Cold Neutron Source
Covering Period:	August 1, 2005 through July 01, 2006
Date of Report:	October 2007
Recipient:	The Regents of the University of California UCD Office of the Vice Chancellor for Research 410 Mrak Hall, One Shields Avenue Davis, CA 95616
Award Number:	DE-FG07-03ID14499
Contact:	Robert G. Flocchini, Director 916.614.6200 rgflocchini@ucdavis.edu Deena M. Bynoe, Associate Director 916.640.1901 dbynoe@ucdavis.edu
Project Team:	Nancy Elizondo, DOE Project Officer 208.526.4169

Development of a Large-Field Cold Neutron Source at the University of California, Davis, McClellan Nuclear Radiation Center (UCD/ MNRC)

R. Flocchini, H. Liu, and M. Boussoufi

Contents

1.0 Introduction

1.1 Significance of Cold Neutrons for Non-Destructive Testing

By comparison with thermal neutrons, cold neutrons are attenuated to a greater extent by elements such as H, O, N, B, Cd, Gd and to a lesser extent by metals such as Be, Al, Fe, Zr, Sn, W, Bi, Pb. Such unique nuclear properties to interact with materials enable to provide better non-destructive inspections.

There are only a few cold neutron sources based on research reactors in the U.S. (Texas, 1 MW; NIST, 20 MW) These cold neutron beams are typically few inches in diameter and primarily used for basic scientific research. Our development of a filtered cold neutron source offers the possibility of a much larger field, approximately up to 20" in diameter, besides competitive source quality. The attempt of such a cold neutron source will be unprecedented in the U.S. and the completed project would offer a great opportunity to accomplish more sophisticated tasks in the automotive, aerospace, and materials science areas, which were unable to investigate with our current neutron radiography facilities.

There is a great need in the aerospace industry for a technique of this type to investigate large and thick castings, which cannot be inspected by X-ray radiography. This is particularly true when the material causing the problem is a low atomic weight element such as hydrogen. NASA's Solid Rocket Booster program has a number of large and thick structural members that would benefit from our intended development of a large-field cold neutron source for inspections. The increased sensitivity of cold neutrons to the presence of hydrogen (total neutron cross section about 30 barns at 0.1 eV to about 80 barns at 0.005 eV) provides a better method for finding very low levels of hydrogen embrittlement in jet engine blades. The U.S. Air Force and commercial airline companies would benefit from identifying this serious problem if our intended development would be made. The automotive industry would also benefit from our development to inspect the internal workings of thick transmission cases for low atomic weight materials, which can only be enhanced by inspections with cold neutrons.

Since the large-field cold neutron source would work synergistically with the rest of MNRC's thermal neutron beams, it is possible to use the dynamic imaging capability to look at two-phase flow with higher contrast and resolution than present systems can accomplish. This capability can be used to investigate a number of valve flow conditions in nuclear reactors. In addition, the neutron tomography imaging system can also utilize cold neutrons to improve and study flow restriction conditions in very small passages.

1.2 Background of Cold Neutrons

The neutron source from existing graphite end plug inside so-called graphite insert consists of merely 1.70% cold neutrons (E_n < 0.005 eV, or 5 meV) and 98.3% non-cold thermal neutrons with energies up to 0.1 eV when thermal neutrons reach an equilibrium temperature around 295 ^oK. This is consistent with both the results calculated from MCNP simulation using 300 ^oK continuous neutron cross-section data and the following equation[1].

$$\mathbf{n_c / n_{th} = 1 - [\ 1 + (\lambda_T/\lambda_c)^2\ ]\ \ exp\ -(\lambda_T/\lambda_c)^2}$$

Where n_c = cold neutrons,
n_{th} = all thermal neutrons,
λ_c = cutoff wavelength for the filter (4.045 A^o or 0.005 eV neutrons for Be, see Figure 1a/1b), and
λ_T = wavelength at temperature T, λ (= 0.286 / $E_{eV}^{1/2}$ A^o).

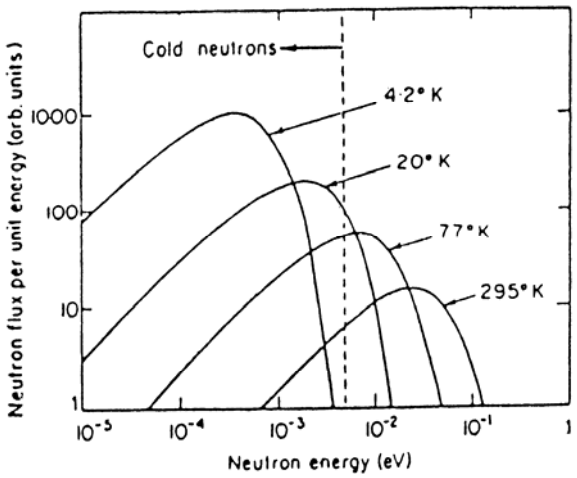

Figure 1a. Maxwell distribution of fluxes for low moderator temperatures.

It is quite clear that even a small leakage of unwanted, but much more numerous, non-cold thermal neutrons incident on a filter may result in more thermal neutrons than desired filtered cold neutrons in the final beam. The practical way to reduce the leakage of non-cold thermal neutrons through a filter is to increase the fraction of cold neutrons incident on the filter. This can be made by placing cryogenic moderator (liquid-hydrogen-cooled or low-temperature solid mesitylene source end) near the reactor core and installing cooled polycrystalline beryllium filter in the beam path.

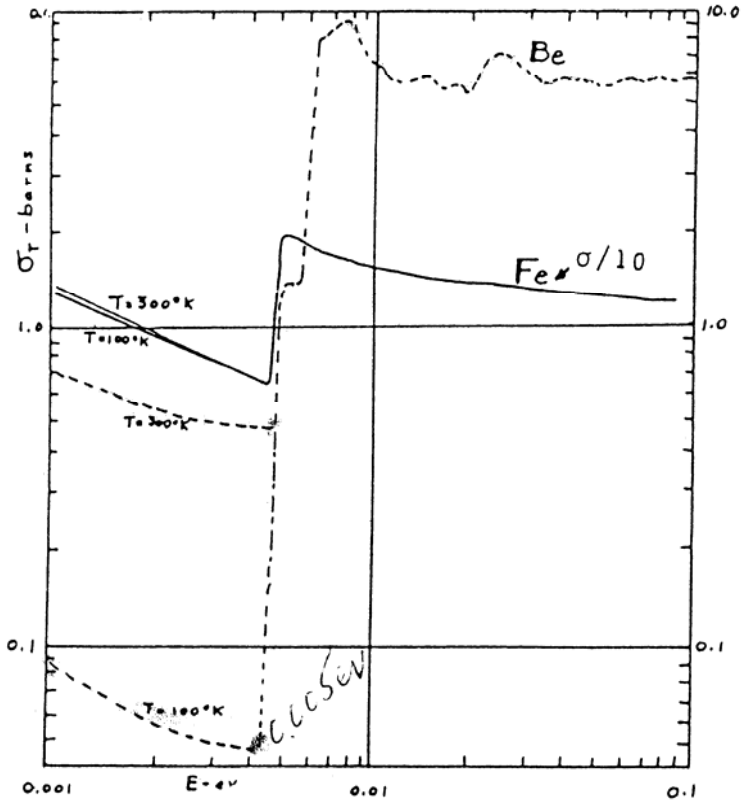

Figure 1b. Total cross sections for slow neutrons, showing the Bragg breaks for Be and Fe near 0.005 eV.

Based on our existing facility configuration, we investigate and study these approaches to develop a large-field, filtered cold neutron source for ongoing research activities with neutron radiography at the MNRC's Bay 3. With an optimal design, the resulting beam of cold neutrons should lead to a minimal leakage from the high-energy tail of thermal neutron spectrum to the final beam.

Table 1 lists the fraction (n_c/ n_{th}) of cold neutrons below 0.005 eV (λ_c = 4.045 A^o) in a thermal neutron beam at various equilibrium temperatures. For a liquid-hydrogen-cooled source end, the "theoretical" fraction of cold neutrons will reach 78.56% while in reality, if an equilibrium temperature around 60 ^{o}K was achieved, this fraction is significantly reduced to 25.21%. On the other hand, if a liquid-nitrogen-cooled source end was implemented and an equilibrium temperature around 100 ^{o}K was reached, the fraction is now dropped to 11.54%. Though, this is still a much higher fraction compared to an equilibrium temperature at 295 ^{o}K under a normal operation condition, which only 1.700% of cold neutrons are available for beam extraction.

Table 1. Fraction of cold neutrons at various equilibrium temperatures.

	20 ^{o}K	60 ^{o}K	77 ^{o}K	100 ^{o}K	295 ^{o}K
E_n (eV)	0.001723	0.005170	0.006635	0.008617	0.02542
λ_T (A^o)	6.889	3.978	3.511	3.081	1.794
n_c/ n_{th} (%)	78.56	25.21	17.46	11.54	1.700

2.0 Neutronic Design

Monte Carlo code MCNP[2-5], version 5 with ENDF B/VI continuous neutron cross sections, is used for the neutronic design study of a large-field cold neutron source at the UCD/ MNRC. Two Pentium-IV PCs are used to run design simulations. Measurements with thermal and threshold activation foils are used to benchmark the integrated neutron flux intensities at the film or imaging location, i.e. 221" away from the beam aperture (2.21" in diameter) of existing beam tube at the MNRC's Bay 3.

Firstly, a detailed simulation with a heterogeneous reactor core is made to include the in-tank and tank-wall sections of existing beam tube at the MNRC's Bay 3. The neutron flux intensities and spectra, calculated from lengthy MCNP's K_{eff} code runs, for the neutron source end, i.e. 1"-thick single crystal bismuth, inside graphite end plug are obtained. Once validated by measured results, these calculated data are used to simulate a fixed neutron source for Monte Carlo runs starting from graphite end plug for subsequent evaluations of beam parameters at the film location.

Secondly, the simulated neutron source is then used to assess a filtered cold neutron source with liquid-nitrogen-cooled polycrystalline beryllium filter placed in the beam tube section inside biological shielding. This is considered as the first design concept.

Thirdly, to further enhance the cold neutron source, the existing graphite end plug is redesigned and evaluated to include a liquid-hydrogen cold trap with polycrystalline beryllium filter. This is considered as the second design concept.

The following discussions will explain the findings and evaluations from both design concepts. Optimized designs for a large-field cold neutron source at the UCD/ MNRC are then proposed for further evaluations.

2.1 Benchmark Comparisons of Existing Beam Tube at Bay 3

Table 2 lists the thermal neutron beam intensity (E_n < 0.1 eV) at the center of the film position 221" away from the beam aperture. Beam quality is defined as the same as the fraction of cold neutrons and beam uniformity is defined as the percentage of flux intensity at 10" away when compared to the center as 100%.

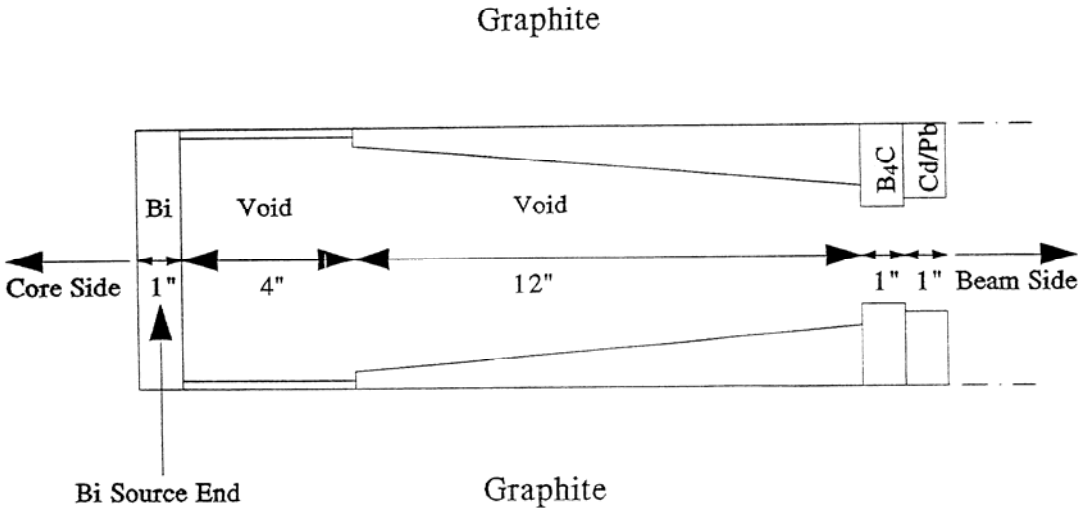

Figure 2. Original design of the existing end plug inside graphite insert.

Table 2. Beam parameters at the film position of Bay 3, reactor at 2.0 MW operating power.

	Beam Intensity ($n/cm^2.sec$)	Beam Quality	Beam Uniformity
Measurement	1.80×10^7	---	95%
Simulation	1.71×10^7	1.71%	94%†

† At >90% probability (confidence) level.

The existing beam aperture for Bay 3 is 2.21" in diameter. Therefore, the L/D ratio (L/D, a measure of the beam path length divided by the aperture that defines the beam) is 100 at the 221"-away film position. Figure 2 illustrates the existing end plug inside graphite insert for Bay 3. Table 2 shows that the consistency between the Monte Carlo computations and the neutron flux measurements is established. Validated data are then used to simulate a fixed neutron source for Monte Carlo runs starting from graphite end plug for subsequent evaluations of beam parameters at the film location. Same

approach is used for both of the design concepts in the following sections. All the flux intensity data in the following evaluations have an estimated statistical uncertainty of < 10%.

2.2 Cooled Polycrystalline Beryllium Filter/ Single Crystal Bismuth Shield for Existing Beam Tube at Bay 3

The existing flux intensity is 1.80 x 10^7 n/cm^2.sec at L/D = 100 location. Considering only 1.70% of cold neutrons in the thermal spectrum at 295 ^oK, a perfect filter without any loss of cold neutrons would deliver a cold neutron source of intensity reaching a maximum value of 3.0 x 10^5 n/cm^2.sec.

Polycrystalline beryllium filter[6] (Figure 1a/1b) is believed to offer excellent filtration of a thermal spectrum with a cutoff energy of 0.005 eV. When polycrystalline beryllium of at least 8" in length is cooled to 77 ^oK (liquid-nitrogen temperature), it produces insignificant loss of cold neutrons but a substantial reduction in the unwanted, non-cold thermal neutron leakage. The total neutron cross section falls abruptly to about 0.6 b for neutrons with energy below 0.005 eV from a rather constant cross section of about 6.0 b for polycrystalline beryllium at room temperature. While 0.6 b is rather small, it is still large enough to limit the useful thickness of polycrystalline beryllium filter. However, when the polycrystalline beryllium is cooled down to 77 ^oK, the transmission of cold neutrons dramatically increases since the total neutron cross section falls further to about 0.06 b.

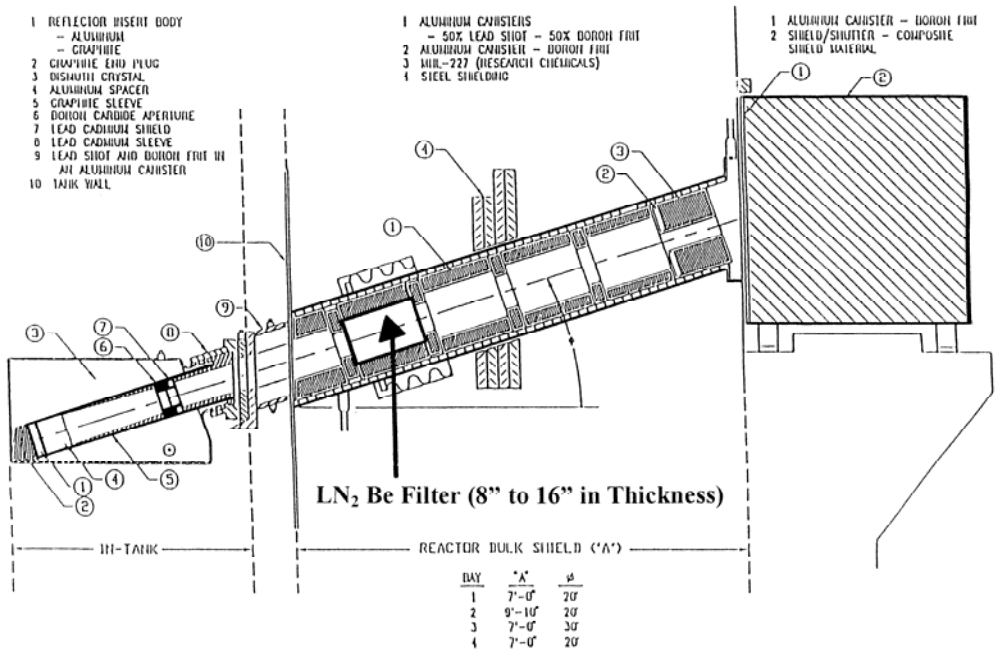

Figure 3. Beam tube section inside biological shielding with cooled polycrystalline beryllium of various thickness and 2"-thick single crystal bismuth. An alternative design would be 24"-thick polycrystalline beryllium without any use of single crystal bismuth.

To validate the above observation, a specially prepared polycrystalline beryllium total neutron cross-section data set at 77 ^{o}K[5] for code MCNP is obtained from Los Alamos National Laboratory. An evaluation is made to assess the impact of installing cooled polycrystalline beryllium of various thicknesses ranging from 8 to 16, then 24 inches in the beam tube section inside biological shielding as seen in Figure 3.

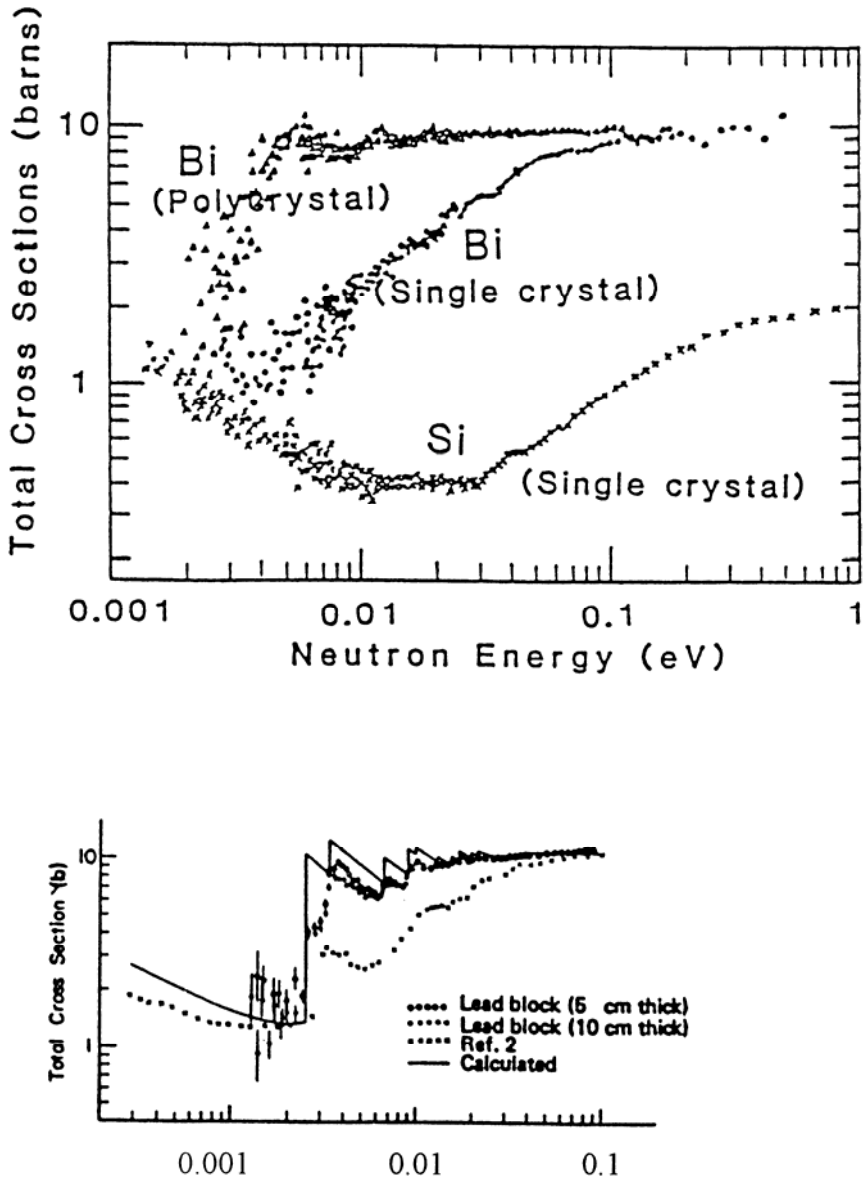

Figure 4a. Comparison of total neutron cross section between polycrystalline and single crystal bismuth at 300 ^{o}K.

The polycrystalline beryllium filter removes the majority of all neutrons with energies above 0.005 eV. On the other hand, to maintain beam quality of similar or lower

gamma contamination level, single crystal bismuth is needed to provide additional gamma shield. Figure 4a shows the total neutron cross section of both polycrystalline and single crystal bismuth at normal temperature 300 ^{o}K. There is a clear advantage of using single crystal bismuth for additional transparency to cold neutrons. It is also believed that "cooled" single crystal bismuth would further enhance such transparency for cold neutrons.[7] Unfortunately, this specific data set is being studied and prepared by the Los Alamos group and will not be available for code MCNP soon due to more complex crystalline structures. Figure 4b shows the plot for Bi-209 (n, total) at 300 ^{o}K from ENDF B-VI (printout from National Nuclear Data Center at Brookhaven National Laboratory) and clearly indicates that the "uncorrected" total neutron cross section data for cold neutrons < 0.005 eV are near and climb above 10 b for lower neutron energies. This data set is apparently not suitable for design simulation and will cause a dramatic reduction of cold neutron transmission. Separate simulation studies show 2"-thick bismuth shield could cut flux intensity of cold neutrons down to a quarter. This is also verified by estimating cold neutron flux through one-dimensional transmission. If "corrected" data at 300 ^{o}K as seen in Figure 4a are used for estimate, the reduction becomes 14%. All the simulation results in the following ignore this reduction of flux intensity due to bismuth addition. It is noted that all the flux intensities of cold neutrons for designs including 2"-thick single crystal bismuth could be 14% overly estimated.

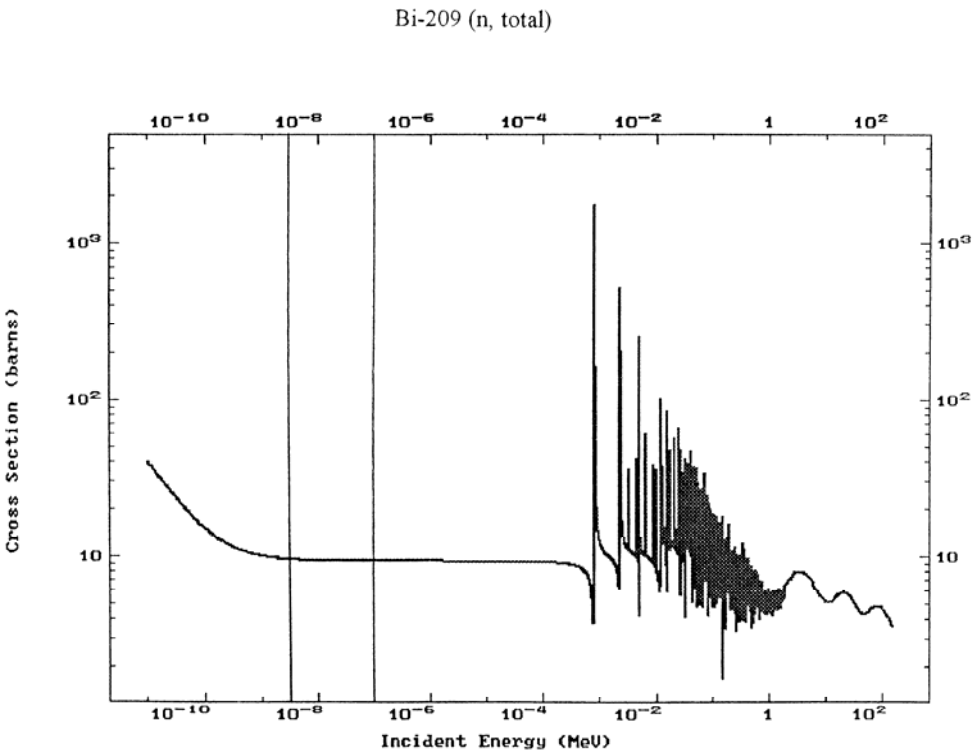

Figure 4b. Total neutron cross section for Bi-209 (n, total) reaction at 300 ^{o}K.

Table 3. Beam parameters at the film position of Bay 3 for designs with cooled polycrystalline beryllium filter of various thicknesses and 2”-thick single crystal bismuth shield, reactor at 2.0 MW operating power.

Filter Thickness	Beam Intensity ($n/cm^2.sec$)	Beam Quality	Beam Uniformity
08” Be + 2” Bi	$2.6 \times 10^{5*}$	˜84%	˜91%†
12” Be + 2” Bi	$2.5 \times 10^{5*}$	˜86%	˜91%†
16” Be + 2” Bi	$2.4 \times 10^{5*}$	˜87%	˜92%†
24” Be	2.1×10^{5}	˜90%	˜92%†

* Could be 14% overly estimated.
† At >90% probability (confidence) level.

When cooled polycrystalline beryllium filter of various thicknesses and 2”-thick single crystal bismuth shield are added in the beam tube section inside biological shielding (Figure 3), the simulation results are shown in Table 3. The cold neutron flux intensity would be about 2.5×10^5 $n/cm^2.sec$ with a beam quality >84%. This flux intensity is about 83% of the maximum value without attenuation. Beam uniformity is considered to be close to what has been achieved for the existing facility.

Table 4. Comparison of beam parameters of cold neutron sources between DIDO and MNRC.

Facility	Beam Intensity ($n/cm^2.sec$)	L/D Ratio	Beam Uniformity
DIDO	3.3×10^{5}	300	> 80%
MNRC	$2.5 \times 10^{5*}$	100	> 85%†

* Could be 14% overly estimated.
† At >99% probability (confidence) level.

To validate the above design evaluation, a comparison (see Table 4) is made to a similar design over the partly decommissioned DIDO reactor[7] in Harwell, U.K. The cold neutron beam over there installs 12”-thick polycrystalline beryllium inside a radial beam tube. The need for gamma contamination reduction is substantially higher for a radial beam tube, therefore 9”-thick single crystal bismuth is used as a gamma shield. Both beryllium filter and bismuth shield are cooled by liquid nitrogen. Their final beam has a flux intensity of 3.3×10^5 n/cm^2.sec and uniformity better than 20% over a 14” diameter. The L/D ratio is 300, which enables very high definition, large area radiographs to be obtained on both static and dynamic equipment.

DIDO reactor is operated at 25 MW operating power compared to MNRC’s 2.0 MW operating power. This major operating power difference, together with the advantage of using heavy water as a reflector over at DIDO, adequately accounts for a much better L/D ratio (300 vs. 100) and a higher flux intensity (3.3×10^5 vs. 2.5×10^5 n/cm^2.sec) of their cold neutron beam. This direct comparison provides credible validation of the design computations.

The loss of beam intensity from the current level of 1.80×10^7 to 2.5×10^5 n/cm^2.sec is a factor of 72. The combined shield of 12”-thick polycrystalline beryllium and 2”-thick single crystal bismuth will provide a shielding factor of 90 for 2 MeV gamma rays. Therefore, the ratio of gamma contamination level to useful neutron flux intensity would be somewhat reduced and improved for the final beam.

As an alternative for additional gamma shielding requirement to maintain the beam quality, an option is to increase polycrystalline beryllium filter to 24” in thickness without any use of single crystal bismuth. In this case, the shielding factor for 2 MeV gamma rays becomes 85, which is still quite adequate for the design. Table 3 shows the results for this alternative design and the flux intensity of cold neutrons is reduced to 2.1×10^5 n/cm^2.sec. However, thicker polycrystalline beryllium filter improves beam quality (fraction of cold neutron) to near 90%.

2.3 Cold Trap and Polycrystalline Beryllium Filter/ Single Crystal Bismuth Shield for Existing Graphite Insert at Bay 3

To obtain a cold neutron fluence of 1 x 10^9 n/cm^2 reaching a film for an optical density of around 2.5 in our current practice as an estimate, it will take an imaging time of 67 minutes, or over an hour, for a beam intensity of 2.5 x 10^5 n/cm^2.sec. To further enhance such a cold neutron source, the existing graphite end plug must be redesigned to include a cryogenic cold trap. A liquid-hydrogen cold trap that would provide the near-maximum cold neutron fraction is evaluated with polycrystalline beryllium filter and single crystal bismuth shield in the following. Other designs of different cryogenic agents can be substitutes with lesser performance simply due to a higher equilibrium temperature, i.e. a smaller fraction of cold neutrons.

Figure 5 illustrates such a design to replace existing graphite end plug. Various thicknesses of polycrystalline beryllium ranging from 8 to 16 inches are evaluated although up to 12" in thickness is about the maximum length existing graphite insert can accommodate. The thicknesses across the beam tube's 6" diameter are 1/16" (Al) + 2/16" (vacuum) + 1/16" (Al) + 11/16" (LH_2) + 1/16" (Al) + 4" (void or Be) + 1/16" (Al) + 11/16" (LH_2) + 1/16" (Al) + 2/16" (vacuum) + 1/16" (Al) as seen in Figure 5. Liquid hydrogen (LH_2) has a physical density of 0.07 g/cm^3, 50/50 ortho/ para content chosen, and both polycrystalline beryllium and single crystal bismuth are cooled by liquid hydrogen.

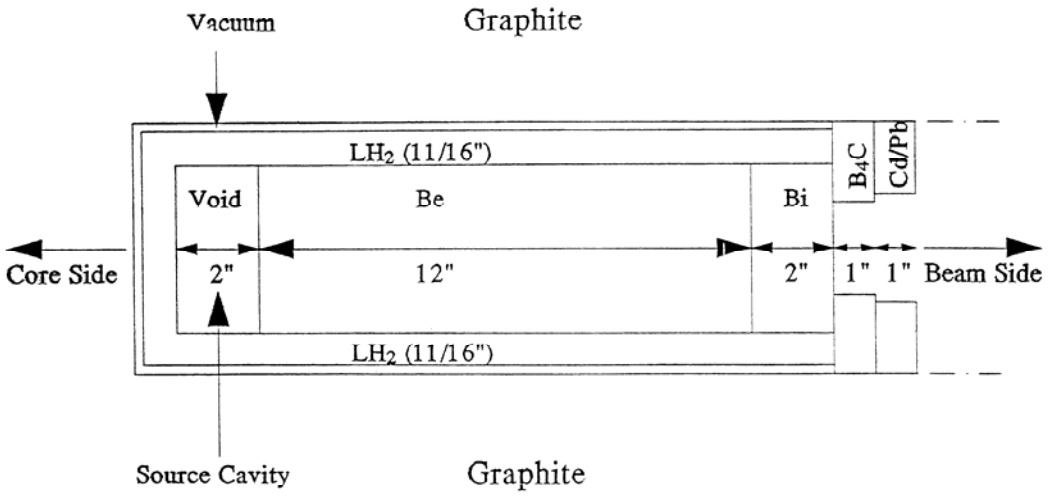

Figure 5. Modified design for the end plug to accommodate a liquid-hydrogen cold trap with 8"-12" thick polycrystalline beryllium filter and 2"-thick single crystal bismuth shield inside graphite insert. An alternative design would be 14"-thick polycrystalline beryllium without any use of single crystal bismuth.

The simulation results are seen in Table 5. Based on the K_{eff} code computations, the designed graphite insert with a LH_2 cold trap, compared to the existing one, would impose an operation reactivity loss of about 8 ± 3 ¢, which is quite insignificant.

The cold neutron flux intensity would be about 4.0 x 10^6 n/cm^2.sec with a beam quality >85%. Beam uniformity is considered to be close to what has been achieved for the existing facility. Both beam quality and uniformity are competitive to the first design. For an intensity of 4.0 x 10^6 n/cm^2.sec, it takes about < 5 minutes to reach a cold neutron fluence of 1 x 10^9 n/cm^2 on a film, which is a significant increase of flux intensity by a factor of 16 compared to the previous design.

The loss of beam intensity from the current level of 1.80 x 10^7 to 4.0 x 10^6 n/cm^2.sec is a factor of 4.5. The combined shield of 12"-thick polycrystalline beryllium and 2"-thick single crystal bismuth (though, 1" additional to the existing design) will provide a shielding factor of 28 for 2 MeV gamma rays. Therefore, the ratio of gamma contamination level to useful neutron flux intensity would be significantly reduced and improved. By increasing the thickness of polycrystalline beryllium to 14" without any us of single crystal bismuth, the reduction for 2-MeV gamma shield becomes a factor of 4.2, which is still quite competitive to current level.

Table 5. Beam parameters at the film position of Bay 3 for designs with liquid-hydrogen cold trap, polycrystalline beryllium filter of various thicknesses and 2"-thick single crystal bismuth, reactor at 2.0 MW operating power.

Filter Thickness	Beam Intensity (n/cm^2.sec)	Beam Quality	Beam Uniformity
08" Be + 2" Bi	4.2 x 10^{6*}	˜85%	˜91%†
12" Be + 2" Bi	4.0 x 10^{6*}	˜87%	˜91%†
16" Be + 2" Bi	3.9 x 10^{6*}	˜88%	˜92%†

* Could be 14% overly estimated.

† At >90% probability (confidence) level.

Study continues to examine a design with two separate systems, i.e. the cold trap in existing graphite insert and cooled filter/ shield in existing beam tube inside biological shielding. The simulation results yield no significant improvement compared to the second design with both the cold trap and the cooled filter/ shield in existing graphite insert.

Figure 6 shows the thermal spectra of both designs at their source ends (bismuth for the first design and void for the second design). The fraction of cold neutrons with a cutoff energy of 0.005 eV, based on the simulation with or without liquid hydrogen, is 1.71% and 29.2%, respectively. For the second design with a 29.2% fraction of cold

neutrons, this implicates that an equilibrium temperature of about 50-60 ^{o}K (see Table 1) is reached for the designed system. The ratio of 29.2% vs. 1.71% is a factor of 17, which approximately explains the difference of extracted flux intensities of cold neutrons (a factor of 16) with or without a liquid-hydrogen cooled source end.

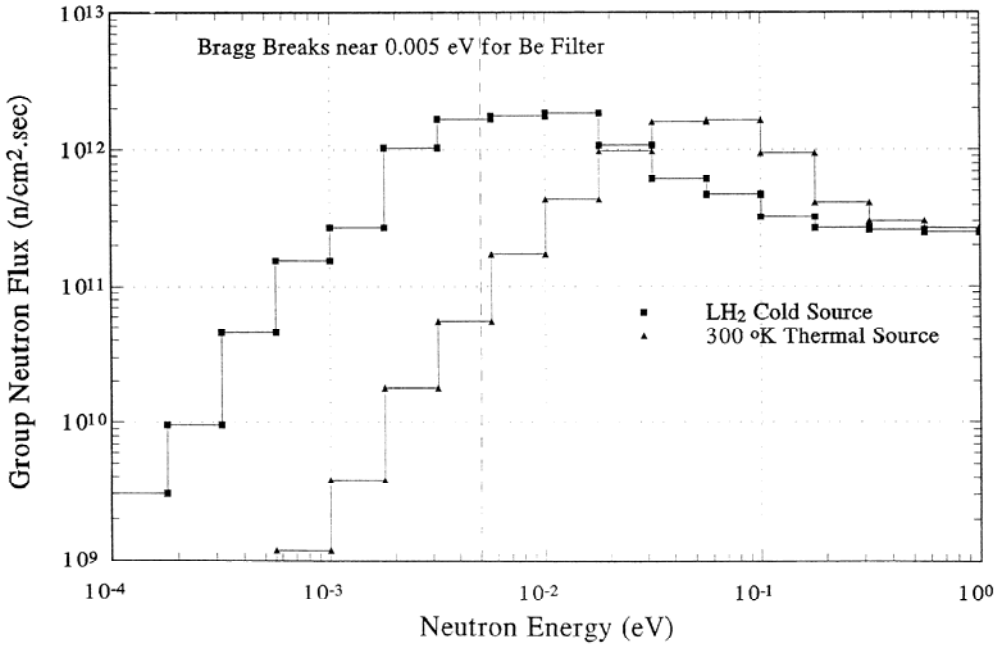

Figure 6. Simulated neutron source spectra of both current (thermal) and modified (cold, LH_2) graphite insert.

Table 6. Flux intensity of cold neutrons based on different cryogenic agents, reactor at 2.0 MW operating power.

	Liquid Hydrogen	Liquid Nitrogen	Solid Mesitylene	Normal Temp.
Temperature (^{o}K)	60	100	228	295
n_c/ n_{th} (%)	25.2	11.5	2.74	1.70
Flux Intensity (n/cm^2.sec)	4.0 x 10^6	1.8 x 10^6	4.1 x 10^5	2.5 x 10^5

A cryogenic system using solid mesitylene as cold moderator, which freezes at 228 ^{o}K, is implemented at the University of Texas. The system is definitely safer and simpler but it has a much lower fraction of cold neutrons to start with. At 228 ^{o}K, the cold fraction is calculated to be 2.74%, which is 60% higher than the equilibrium value at normal temperature 295 ^{o}K but only 11% of a liquid-hydrogen cooled system. The low

neutron efficiency for a mesitylene-cooled system is obvious compared to a cryogenic system with liquid hydrogen or nitrogen.

By using the fraction of cold neutrons at various equilibrium temperatures to interpolate for flux intensities of cold neutrons with the same filter and shield design, Table 6 lists the estimate flux intensity of cold neutrons for a system using liquid nitrogen or solid mesitylene as a cryogenic agent. Due to the limitation of computing speed with PCs, spectral evaluation of different cryogenic agents becomes unrealistic within reasonable run times. Therefore, integrated flux intensities of cold neutrons are used to compare for the neutron efficiency of each design.

3.0 Heat Load Evaluation

3.1 Monte Carlo Evaluation

MCNP is then used to estimate the energy deposited in the designed graphite insert as seen in Figure 5. The code directly tallies the prompt contributions, i.e. fast neutrons, fission and prompt gamma rays, to the heat load. A separate evaluation was made to assess the heat load added to the graphite insert for the second design concept while the heat load added to the cooled filter in the first design concept can be easily managed. The energy deposited in the graphite insert are summarized in Table 7. The calculated total heat load is about 270 watts based on 2 MW operating power.

Table 7. Nuclear heating in watts in the designed graphite insert seen in Figure 5.

	LH_2 (220 g)	Al (3000 g)	Be (4500 g)	Bi (4000 g)
Fast Neutrons	58	2	29	0
Gamma Rays	9	70	75	27
Total (Watt)	67	72	104	27

3.2 Conclusion

In summary, to enhance the neutron radiography capability at the UCD/ MNRC, a neutronic design study for a large-field cold neutron source is made for MNRC's Bay 3. Two optimized designs are concluded from the above sections.

The first design is based on cooled either 12"-thick polycrystalline beryllium filter and 2"-thick single crystal bismuth shield or 24"-thick polycrystalline beryllium filter alone for existing beam tube at Bay 3. This conservative design to generate a filtered cold neutron source would deliver a flux intensity of cold neutrons about 2.1 ~ 2.5 x 10^5 n/cm^2.sec at L/D =100 location.

To significantly increase the source of cold neutrons for the second design, a cold trap together with either 12"-thick polycrystalline beryllium filter and 2"-thick single crystal bismuth shield or 14"-thick polycrystalline beryllium alone is designed for existing graphite insert at Bay 3. Based on using liquid hydrogen as a cryogenic agent to achieve an equilibrium temperature around 60 ^{0}K, the cold neutron flux would increase to 4.0 x 10^6 n/cm^2.sec at L/D = 100 location. Both designs would offer the possibility of a much larger field, approximately up to 20" in diameter, besides competitive source quality, i.e. high fraction of cold neutrons and beam uniformity.

By using the fraction of cold neutrons at various equilibrium temperatures to interpolate for flux intensities of cold neutrons with the same filter and shield design, a number of other cryogenic agents are evaluated for their cold neutron production efficiency, including liquid nitrogen and solid mesitylene. Since using liquid hydrogen would offer the best beam parameters in the second design concept, we continue to evaluate its engineering issues based on the calculated heat load of about 270 watts. The actual equilibrium temperature and the fraction of cold neutrons are heavily dependent on the performance of a specific cryogenic system and the mechanical design.

4.0 References

1. W. Whittemore and H. Berger, “Physics of Neutron Radiography Using Selected Energy Neutrons,” Neutron Radiography, edited by J. Barton *et al.*, pp. 23-33, Brussels and Luxembourg, 1983.

2. Neutron Cross Sections, Volume 1, Neutron Resonance Parameters and Thermal Cross Sections, edited by S. Mughabghab *et al.*, National Nuclear Data Center, Brookhaven National Laboratory, published by Academic Press.

3. Neutron Cross Sections, Volume 2, Neutron Resonance Parameters and Thermal Cross Sections, edited by V. McLane *et al.*, National Nuclear Data Center, Brookhaven National Laboratory, published by Academic Press.

4. MCNP- A General Monte Carlo N-Particle Transport Code, Version 5, by X-5 Monte Carlo Team, Los Alamos National Laboratory, RSICC Computer Code Collection, April 2003.

5. Neutron cross-section data for polycrystalline beryllium at liquid nitrogen 77 ^{o}K temperature, personal communications w/ R. MacFarlane and E. Pitcher, Los Alamos National Laboratory, Summer 2004.

6. W. Whittemore and Y. Nir-El, “Cold Neutrons for Neutron Radiography,” Neutron Radiography, edited by S. Fujine *et al.*, pp. 145-157, Brussels and Luxembourg, 1983.

7. D. Taylor, “Neutron Radiography at DIDO Reactor,” Neutron Radiography, edited by J. Barton *et al.*, pp. 145-151, Brussels and Luxembourg, 1983.

5.0 Appendix

Partial MCNP input file:

```
MNRC cold neutron source
c
c     A1-  20/20
1     1   -6.51       -1       719  -723
2     22  -6.3         1 -201  719  -723
3     3   -1.6      -201       717  -725 (-719:723)
4     4   -8.032     201 -401  717  -725
5     5   -4.516         -401  711  -731 (-717:725)
c
.....
Heterogeneous core configuration
c
c     ***** ***** ***** ***** ***** ***** ***** ***** *****
c     Reflector side; Modification volume
c     Al compensator; Al and H2O
c
721   8   -2.7  715 -727 781 -783 (-971:974)  $ Al 8 -2.7
722   8   -2.7  971 -974 781 -782 (-972:973)  $ Al 8 -2.7
723   7   -1    972 -973 781 -782
724   7   -1    971 -974 782 -783
c
731   12  -2.7  921 -924     -951 (-922:923:941)  $ Al can, water gap 2 mm
732   12  -2.7  921 -924     -952 (-922:923:942)  $ Al can
733   12  -2.7  921 -924     -953 (-922:923:943)  $ Al can
734   12  -2.7  921 -924     -954 (-922:923:944)  $ Al can
735   12  -2.7  921 -924     -955 (-922:923:945)  $ Al can
736   12  -2.7  921 -924     -956 (-922:923:946)  $ Al can
737   12  -2.7  921 -924     -957 (-922:923:947)  $ Al can
738   12  -2.7  921 -924     -958 (-922:923:948)  $ Al can
c
c     ***** ***** ***** ***** ***** ***** ***** ***** *****
741   14  -2.42     922 -923     -931
742   14  -2.42     922 -923     -932
743   7   -1        922 -923     -933
744   7   -1        922 -923     -934
745   9   -0.0013   922 -923     -935
746   9   -0.0013   922 -923     -936
747   7   -1        922 -923     -937
748   7   -1        922 -923     -938
c
751   14  -2.42     922 -923         931 -941
752   14  -2.42     922 -923         932 -942
753   7   -1        922 -923         933 -943
754   7   -1        922 -923         934 -944
755   9   -0.0013   922 -923         935 -945
756   9   -0.0013   922 -923         936 -946
757   7   -1        922 -923         937 -947
758   7   -1        922 -923         938 -948
c
761   7   -1       -951              715 -727 (-921:924)
762   7   -1       -952              715 -727 (-921:924)
763   7   -1       -953              715 -727 (-921:924)
764   7   -1       -954              715 -727 (-921:924)
765   7   -1       -955              715 -727 (-921:924)
766   7   -1       -956              715 -727 (-921:924)
767   7   -1       -957              715 -727 (-921:924)
768   7   -1       -958              715 -727 (-921:924)
c
771   8 -2.7  600  965 -966 783 -786 715 -727  951 952
772   8 -2.7  600  965 -966 786 -787 715 -727  951 952
773   7 -1    600  966  968 783 -787 715 -727
774   8 -2.7  599  967 -968 783 -786 715 -727  953 954
775   8 -2.7  599  967 -968 786 -787 715 -727  953 954
776   7 -1   -600  966 -967 783 -787 715 -727
777   8 -2.7 -600  965 -966 783 -786 715 -727  955 956
778   8 -2.7 -600  965 -966 786 -787 715 -727  955 956
779   7 -1   -600 -965 -967 783 -787 715 -727
780   8 -2.7 -599  967 -968 783 -786 715 -727  957 958
```

```
781   8 -2.7 -599  967 -968 786 -787 715 -727  957 958
782   7 -1    600  968 -965 783 -787 715 -727
c
783   7 -1    715 -727 787 -791
c
c     reflector top H2O
784   7 -1    727 -741 781 -791
c
c     reflector bottom H2O
785   7 -1    705 -715 781 -791
c
c     ***** ***** ***** ***** ***** ***** ***** ***** *****
c     TNR cold neutron source term
c
791   9  -0.0013       983 -984 -993
792   8  -2.7          982 -984 -992 #791
793   16 -0.07         981 -984 -991 #791 #792
794   17 -1.85         984 -985 -993
795   8  -2.7          984 -985 -992  993
796   16 -0.07         984 -985 -991  992
797   10 -9.8          985 -986 -994
798   8  -2.7          985 -986  994 -991
799   9  -0.0013       986 -987 -995
800   11 -2.49         986 -987  995 -991
801   9  -0.0013       987 -988 -996      -779  -725
802   13 -10.0         987 -988  996 -991 -779  -725
803   9  -0.0013            988      -991 -779  -725
c
c     ***** ***** ***** ***** ***** ***** ***** ***** *****
c     Central Al tube: Irradiation facility
c     CIF..... w/ graphite plug
c
831   7   -1      902 -903 705 -711
832   23  -1.66   902 -903 711 -731
833   7   -1      902 -903 731 -741
834   7   -1      901 -902 705 -711
835   8   -2.7    901 -902 711 -741
836   7   -1          -900 705 -822
837   7   -1          -900 822 -823
838   7   -1          -900 823 -824
839   7   -1          -900 824 -719
c
811   7   -1          -900 719 -800  $
812   7   -1          -900 800 -801  $ -7
813   7   -1          -900 801 -802  $ -6
814   7   -1          -900 802 -803  $ -5
815   7   -1          -900 803 -804  $ -4
816   7   -1          -900 804 -805  $ -3
817   7   -1          -900 805 -806  $ -2
c     7   -1          -900 806 -807  $
818   7   -1          -900 806 -809  $ Center
c     7   -1          -900 808 -809  $
819   7   -1          -900 809 -810  $  2
820   7   -1          -900 810 -811  $  3
821   7   -1          -900 811 -812  $  4
822   7   -1          -900 812 -813  $  5
823   7   -1          -900 813 -814  $  6
824   7   -1          -900 814 -815  $  7
825   7   -1          -900 815 -723  $
826   7   -1          -900 723 -741
827   7   -1      900 -901 705 -741
888   8 -2.7      903 -905 711 -731
999   0           (-705:741:791)

1     c/z    -22.61616     -8.70712     0.3175  $ Zr rod
.....
c
705   pz    -80
707   pz    -76.2
709   pz    -73.66
711   pz    -37.465
713   pz    -34.29
715   pz    -28.8925
717   pz    -27.94
719   pz    -19.05
```

```
723   pz     19.05
725   pz     27.94
727   pz     28.8925
729   pz     29.845
731   pz     33.02
733   pz     41.32
741   pz     80
c
771   cz     15.24
773   cz     26.37
775   cz     26.67
777   cz     27.305
779   cz     60.0075  $ 3/8" Al
781   cz     60.96    $ at 24" radius locations
782   cz     62.1125  $ 3/8" + 2 mm
783   cz     63.265   $ 3/4" + 4 mm
786   cz     69.615   $ 2.5"
787   cz     76.6     $ 69.615 + 2.25" + 0.5"
791   cz     80
c     cz    106.68    $ +0.25" Al tank vessel
c
131   pz    -54.61    $ transient rod
176   pz      3.81
358   pz     57.15
c
151   pz    -43.18    $ 5 fuel-follower control rods
164   pz    -26.67
335   pz     11.43
363   pz     49.53
376   pz     65.96
c
800   pz    -19.04
801   pz    -16.50
802   pz    -13.96
803   pz    -11.42
804   pz     -8.88
805   pz     -6.34
806   pz     -3.80
807   pz     -1.26
c     pz      1.26
809   pz      3.80
810   pz      6.34
811   pz      8.88
812   pz     11.42
813   pz     13.96
814   pz     16.50
815   pz     19.04
c
822   pz    -46.99
823   pz    -26.68
824   pz    -21.59
c
c     Central tube
900   cz       1.3813
901   cz       2.3813
902   cz       2.54     $ 2"-1/16" Al tubing
903   cz       5.08     $ 4" plug
904   cz       5.36     $ 4.22"
905   cz       5.61     $ 4.42"
c
899   c/z     11.30808    -19.59102     0.79375  $ 0.625" inside
911   c/z     11.30808    -19.59102     1.38     $ 1.08" pneumatic tube
490   c/z     11.30808    -19.59102     1.5875   $ 1.25"
c
921   pz    -17.78
922   pz    -13.97
923   pz     11.43
924   pz     15.24
c
931   c/z    69.615    -5.8928   2.54  $ 2.0" I.D. Stuff (Si, H2O, Air)
932   c/z    69.615     5.8928   2.54
933   c/z     5.8928   69.615    2.54
934   c/z    -5.8928   69.615    2.54
935   c/z   -69.615     5.8928   2.54
936   c/z   -69.615    -5.8928   2.54
```

```
937   c/z    -5.8928  -69.615    2.54
938   c/z     5.8928  -69.615    2.54
c
941   c/z    69.615    -5.8928   3.81  $ 3.0" I.D. Stuff (Si, H2O, Air)
942   c/z    69.615     5.8928   3.81
943   c/z     5.8928   69.615    3.81
944   c/z    -5.8928   69.615    3.81
945   c/z   -69.615     5.8928   3.81
946   c/z   -69.615    -5.8928   3.81
947   c/z    -5.8928  -69.615    3.81
948   c/z     5.8928  -69.615    3.81
c
951   c/z    69.615    -5.8928   5.715
952   c/z    69.615     5.8928   5.715
953   c/z     5.8928   69.615    5.715
954   c/z    -5.8928   69.615    5.715
955   c/z   -69.615     5.8928   5.715
956   c/z   -69.615    -5.8928   5.715
957   c/z    -5.8928  -69.615    5.715
958   c/z     5.8928  -69.615    5.715
c
965   py    -12.6078
966   py     12.6078
967   px    -12.6078
968   px     12.6078
c
971   pz    -13.97
972   pz     -8.89
973   pz      6.35
974   pz     11.43
c
c     Drawings: T2Z800 series
981   3 px    0
982   3 px    1.74625
983   3 px    2.54       $ 1/16 Al + 1/8 void +
c                        $ 1/16 Al + (11/16 LH) + 1/16 Al
984   3 px    7.62
985   3 px   38.10       $ 12" Be
986   3 px   43.14       $ 2" Bi
987   3 px   45.72       $ 1" B4C
988   3 px   48.26       $ 1" Pb-Cd
c
991   3 cx    7.62       $ 3" radius
992   3 cx    5.87375    $ 3 - 11/16
993   3 cx    5.08       $ 2"
994   3 cx    6.35       $ 2.5"
995   3 cx    2.8067     $ 2.21" beam aperture
996   3 cx    3.1623     $ 2.49" beam aperture

Transformation 30 degrees
*tr3      0 -34.93 0 30 90 60 90 0 90 120 90 30 1
c
.....
Tally computations
c
f4:n      818 791
fm4       1.5e17
f6:n      796 795 794 797
fm6       2.4e4
c         1.5e17 * 1.6e-13 (w/g)
f16:p     796 795 794 797
fm16      2.4e4
c
m1        40000.66c     1
m2         1001.66c    -0.01500
          40000.66c    -0.85500
          92235.66c    -0.01275
          92238.66c    -0.06800
mt2        zr/h.04t  h/zr.04t
m22        1001.66c    -0.01400
          40000.66c    -0.79800
          92235.66c    -0.03000
          92238.66c    -0.16000
          68166.00c    -0.00114
          68167.00c    -0.00077
```

```
mt22       zr/h.01t  h/zr.01t
m3         6000.66c     1
mt3        grph.01t
m23        6000.66c     1
mt23       grph.01t
m33        6000.66c    -0.8469  $ -1.49
          13027.66c    -0.1531  $ -0.27
mt33       grph.01t
m4        26000.55c    -0.7012
          14000.60c    -0.0050
          24000.50c    -0.1900
          25055.60c    -0.0100
          28000.50c    -0.0925
m5        26000.55c    -0.7012
          14000.60c    -0.0050
          24000.50c    -0.1900
          25055.60c    -0.0100
          28000.50c    -0.0925
           1001.66c    -0.0138
           8016.66c    -0.1105
mt5        lwtr.01t
m6         1001.66c    -0.1111
           8016.66c    -0.8889
mt6        lwtr.01t
m7         1001.66c    -0.1111
           8016.66c    -0.8889
mt7        lwtr.01t
m8        13027.66c    -0.9755
          12000.66c    -0.0100
          14000.60c    -0.0060
          24000.50c    -0.0020
          26000.55c    -0.0035
          29000.50c    -0.0030
m9         7014.66c     0.8
           8016.66c     0.2
m10       83209.66c     1
m11        6000.66c    -0.216
           5010.66c    -0.156
           5011.66c    -0.628
m12       13027.66c   -23
           1001.66c    -0.1111
           8016.66c    -0.8889
mt12       lwtr.01t
m13       82000.50c    -0.5673
          48000.42c    -0.4327
m14       14000.60c     1
m15        6000.66c     0.3333
           1001.66c     0.6667
mt15       poly.01t
m16        1001.66c     1
mt16       hortho.01t
c          hpara.01t
m17        4009.66c     1
mt17       be.00t               $ be77k
phys:p    j  1  1
```

End of File.